ELECTRIC FIELD ENHANCEMENT AND DETERIORATION OF BOILING HEAT TRANSFER AND CRITICAL HEAT FLUX IN DIELECTRIC FLUIDS

P. M. Carrica
V. Masson
Centro Atómico Bariloche
(8400) Bariloche – Argentina

ABSTRACT

We present the results of an experimental study of the effects of externally imposed electric fields on boiling heat transfer and critical heat flux (CHF) in dielectric fluids. The study comprises the analysis of geometries that, under the effects of electric fields, cause the bubbles either to be pushed toward the heater or away from it. A local phase detection probe was used to measure the void fraction and the interfacial impact rate near the heater. It was found that the critical heat flux can be either augmented or reduced with the application of an electric field, depending on the direction of $\nabla\left(\vec{E}\cdot\vec{E}\right)$In addition, the heat transfer can be slightly enhanced or degraded depending on the heat flux. The study of the two-phase flow in nucleate boiling, only for the case of favorable dielectrophoretic forces, reveals that the application of an electric field reduces the bubble detection time and increases the detachment frequency. It also shows that the two-phase flow characteristics of the second film boiling regime resemble more a nucleate boiling regime than a film boiling regime.

INTRODUCTION

It is well known that the application of an electric field near a boiling surface has strong effects in the boiling characteristics, including the heat transfer properties, the near-heater two-phase flow and the critical heat flux. The pioneering works in the subject are now about 30 years old [1-4]. Excellent reviews on electrohydrodynamically enhanced boiling heat transfer can be found in references [5] and [6].

Among the observed effects of the application of an external electric field to a boiling wire heater immersed on a dielectric fluid are the improvement of the heat transfer in the natural convection region [6], a strong increase in the CHF [1, 7], a slight enhancement on the heat transfer coefficient in nucleate boiling [8] and the occurrence of a second film boiling regime with small bubbles that undergoes a second boiling crisis with a transition to the standard film boiling regime [9].

A typical boiling curve covering the three boiling regimes is shown in Fig. 1. This curve was measured by Carrica et al. [9] for a 0.2 *mm* wire in R-113 at saturation temperature. We can clearly identify the development of a third boiling regime, referred to as *Film II* regime in [9], when an electric field is applied. Under the effects of electric fields two boiling crises can be identified: the first boiling crisis (CHF), corresponding to the transition from nucleate boiling to film II, and a second boiling crisis in which there is a transition between film II to the standard film boiling. This second crisis is not present without electric fields.

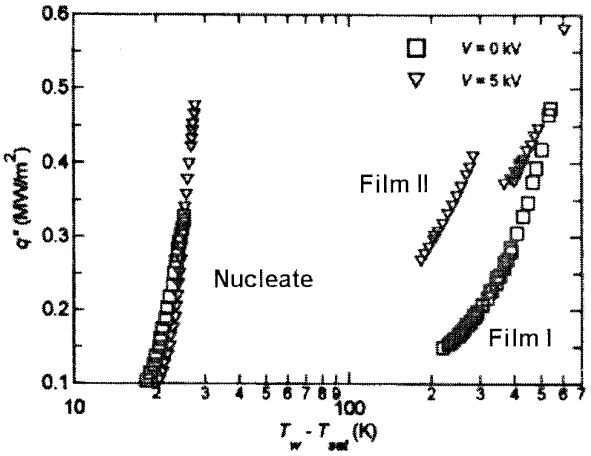

Fig 1 - Typical boiling curves for a 0.2 *mm* wire at 0 and 5 *kV* of applied voltage (from reference [9])

In the natural convection region, the application of an electric field results in the presence of an electrical body force of the form

$$\mathbf{f}_e = \rho_e \mathbf{E} - \frac{1}{2}\varepsilon_o E^2 \nabla\varepsilon + \nabla\left[\frac{1}{2}\varepsilon_o E^2 \rho\left(\frac{\partial\varepsilon}{\partial\rho}\right)\right] \quad (1)$$

where the different terms are related to the presence of free charge and to inhomogeneities in the dielectric constant and in the electric field distribution, caused in this case by thermal gradients. This force can either enhance or inhibit the motion due to natural convection [5]. The consequence is that the heat transfer coefficient in the natural convection regime can, in principle, be increased or decreased by the application of an electric field.

The analysis of the CHF is more complex, and the phenomena involved in this boiling regime transition are not fully understood to the present, even without the application of electric fields. The classical theory of the hydrodynamic instability [10] has been extended to the case when an electric field is applied by Johnson [3]. Under the standard hypotheses that when the vapor jets become unstable the CHF occurs, the CHF with an applied electric field is related to the CHF without field by

$$\frac{q''_{CHF,E}}{q''_{CHF,0}} = \sqrt{\frac{\lambda_{u0}}{\lambda_{uE}}} \quad (2)$$

where λ_{u0} is the most dangerous Taylor wavelength with no electric field applied. The most dangerous Taylor wavelength with an applied electric field λ_{uE} has been found to decrease when increasing the electric field as

$$\frac{\lambda_{u0}}{\lambda_{uE}} = \frac{El^* + \sqrt{El^{*2} + 3}}{\sqrt{3}} \quad (3)$$

where

$$El^* = \frac{\varepsilon_o \varepsilon_{eq} E_I^2 L}{\sigma} \quad (4)$$

is called the electric influence number and is calculated using the value of the electric field at the vapor/liquid interface, E_I, and an equivalent permittivity ε_{eq}

$$\varepsilon_{eq} = \frac{\varepsilon_o \varepsilon_l \left(\varepsilon_l - \varepsilon_g\right)^2}{\varepsilon_g \left(\varepsilon_l + \varepsilon_g\right)} \quad (5)$$

Other forms of Eq. (3) have been given [6], but all show an increase in the CHF when increasing the applied voltage. The hydrodynamic instability model has been found to successfully predict the trend of the CHF experimental data under different conditions [3, 7, 11].

The CHF on several geometries with applied electric fields has been extensively studied. In addition to the already mentioned strong increase in the CHF, it has also been reported a suppression of the transition boiling regime [5]. Experimental studies on the effects of subcooling [7], heat-up rate [12] and reduced gravity [13] have been made in an attempt to learn more about this interesting phenomenon. However, all of these studies deal with heater/electrode geometries in which the dielectrophoretic force pulls the bubbles away from the heater, then helping the liquid renewal at the surface.

The dielectrophoretic force acting on a small bubble immersed in a dielectric fluid with an applied non-uniform electric field $\vec{E}$ is [8]:

$$\vec{F}_c = 2\pi r_b^2 \frac{\varepsilon_g - \varepsilon_l}{\varepsilon_g + 2\varepsilon_l} \varepsilon_o \varepsilon_l \nabla\left(E^2\right) \quad (6)$$

where ε_l and ε_g are the electric permittivities of the liquid and vapor relative to the absolute electric permittivity of vacuum ε The term $\left(\varepsilon_g - \varepsilon_l\right)/\left(\varepsilon_g + 2\varepsilon_l\right)$ is negative, so this force points toward regions of weaker electric field strength. A favorable dielectrophoretic force, in the sense that helps the bubbles leave the heater, is achieved when the electric field strength decreases as we move away from the heater, no matter the field polarity. This is the case of wire heaters with cage-like electrodes. On the other hand, cylindrical heaters with wire electrodes in the axis produce an adverse dielectrophoretic force. It can be expected that an adverse dielectrophoretic force will cause a more difficult vapor removal from the heater.

The effects of the application of electric fields on nucleate boiling heat transfer are by far less important than the effects on CHF. It has been observed a slight increase in the heat transfer coefficient at low heat fluxes and a reduction at high heat fluxes when an electric field is imposed [14]. Other works report the same enhancement on the heat transfer at low heat fluxes, but slight or no effect at all at high heat fluxes. In boiling R113 Uemura et al. [15] found that beyond certain heat flux the electric field has no effect on the heat transfer coefficient. It must be noticed that in reference [14] the heater was a small wire (0.2 *mm* in diameter) while in reference [15] the heater was an horizontal plate.

It has been observed, in addition, that the two-phase flow near the heated surface undergoes abrupt changes in the presence of electric fields [6]. The first quantitative experimental data of the effects of electric fields on the two-phase flow near a heated surface has been published in reference [16].

In this work we present an experimental study of the effect of adverse and favorable electric fields on boiling heat transfer and critical heat flux in a dielectric fluid (R113). The two-phase flow adjacent to a heater wire with and without the application of electric fields has been also studied. The paper is organized so as to show the main features of electric field enhancement and deterioration, and in doing so, some results previously published by the authors are shown, along with new data.

EXPERIMENTAL SETUP

Two heater geometries have been studied: a wire heater with a cage-like electrode and a semi-cylindrical heater with a wire electrode on the axis. In both cases, the test sections were immersed in R113 at saturation temperature inside a stainless steel vessel, 300 *mm* internal diameter, with four lateral windows for visualization of the phenomena. Both experimental sections were used to measure the boiling curves and the critical heat flux.

The liquid temperature was controlled using a 400 *W* electric preheater, and uniformity of the temperature was guaranteed within 1 ^oC and controlled with three K- type thermocouples positioned in different places inside the vessel. A copper coiled condenser, cooled by tap water, was used to condense the vapor back to the pool. A reflux condenser open to the ambient assured atmospheric pressure conditions in all of the experiments (0.92 *bar*, 800 *m* over sea level). The high voltage was provided by a Spellman R10PN power supply, capable of outputs up to 10 *kV*.

The test section used for the wire heater is depicted in Fig. 2. An 8-wire cylindrical cage surrounding the heater was used as the high voltage electrode. The ground electrode was the heater itself. The length of the cage was 120 *mm* to minimize end effects. It has been observed that distortions on the electric field result in the possibility of local CHF that then propagates through the whole heater [7].

The heater was built brazing coaxially a 0.3 *mm* in diameter platinum wire to a 0.8 μm copper wire, a diameter chosen such that the overheating in the copper remains below 1 ^oC over all the current rates in the experiments. Direct sensing of the voltage drop across the heater was attained by welding two thin platinum wires at the copper-platinum junction, as shown in Fig. 2. Again, great care was taken to minimize the size of the welding and sensing wires to avoid distortions on the electric field.

The second heater was constructed as shown in Fig. 3. A platinum foil 25 μm thick was bonded with epoxy to an acrylic substrate semi-cylindrically shaped. The heater diameter was 1.7 *mm*, and the thickness of the substrate (3 *mm*) was calculated to be enough to make negligible the downward heat losses due to conduction. Care was also taken to make the experimental runs slow enough to safely neglect the heat capacity of the substrate. The electrode was made of a thin copper wire (0.25 *mm* in diameter) and was held at the axis of the semi-cylinder, as shown in Fig. 3. Voltage sensing wires were welded to the heater with silver in order to avoid the voltage drop on the power cables, connections, weldings, etc. The welding was made so that the position of the wires match with the radius of the cylinder.

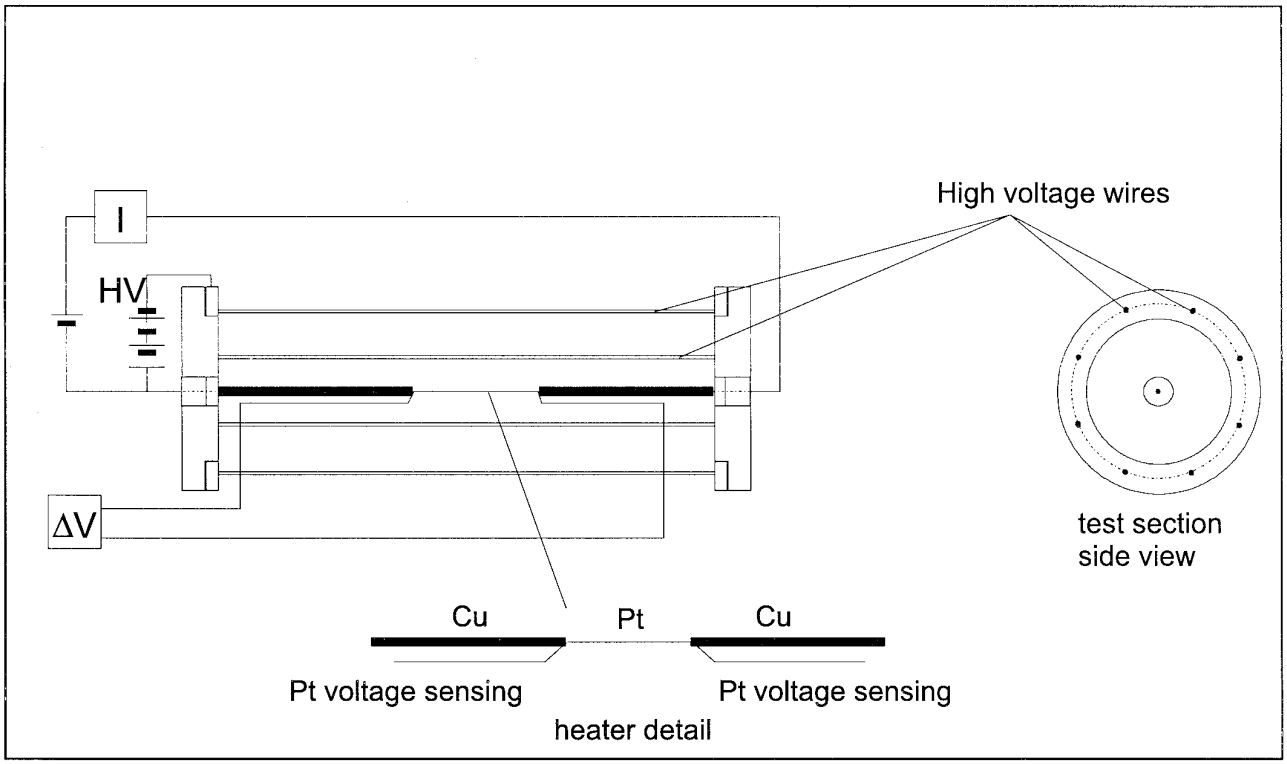

Fig. 2 - Test section and heater details for the favorable dielectrophoretic force case.

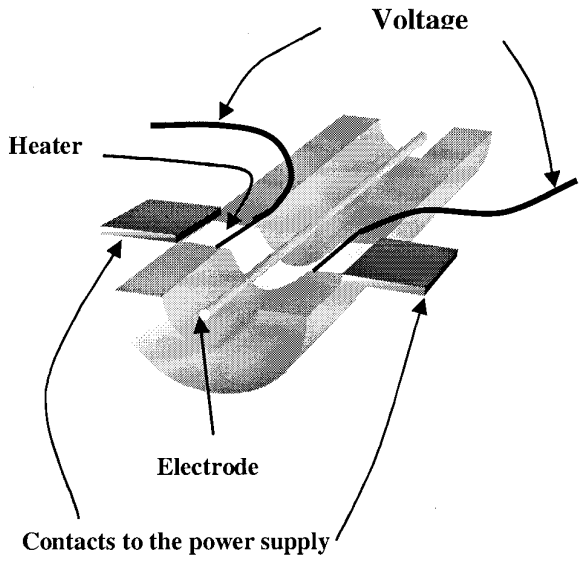

Fig. 3 - Heater details for the adverse dielectrophoretic force case.

A Bruker B-MN 70-700 DC constant-current power supply controlled by a PC computer was used to provide power to the heaters. The control results in a resolution of 0.07 *A*. The current through the heater was measured using a calibrated shunt. Steady state measurements were also possible.

Temperature and heat flux were calculated from the measurements of the voltage drop across the heater and the current through it. In the range of temperatures used in this work, the resistance of the platinum wire follows the law:

$$R = R_o\left(1+\beta\Delta T-\gamma\Delta T^2\right) \qquad (7)$$

where $\Delta T = T - T_{sat}$ is the platinum overheating, T_{sat} is the liquid saturation temperature, $\beta = 3.908\text{x}10^{-3}\ K^{-1}$ and $\gamma = 5.802\text{x}10^{-7}\ K^{-2}$ [17]. The heater resistance at saturation temperature R_0 was calculated after measurements at very low heat flux, where the heater overheating is negligible, using a linear fit with least squares. The calculation of the heater temperature was very sensible to the evaluation of the resistance R_0. Voltage drop across the heater and current through it were measured using a 16-bit A/D plug-in card.

In order to preserve the heaters from high temperature damage we used a Wheatstone-bridge-based CHF detector connected to the high-speed relay of the Bruker power supply. The system detects the heater temperature jump caused by the transition to film boiling and cuts the power to the heater when the rate of change of the heater resistance was higher than a prescribed value. The high speed relay feature of the Bruker power supply was fast enough to disconnect the power and to avoid the decomposition of the refrigerant and the carbon deposition in the heater, caused by high temperature excursions. Carbon deposition also causes the results in CHF to be non-repetitive. In addition, on the cylindrical heater, the high temperature can damage the epoxi bond and the substrate. For all the measurements were film boiling was attained, only the wire heaters were used.

Two-phase flow parameters were measured using a single-tip true-monofiber probe specifically designed for uses on applications were electric fields are present. The construction and assembly of this type of probe has been extensively discussed in references [16] and [18], and only an outline is given here.

The probe was constructed using Mitsubishi ESKA multimode fiber optics, 250 μm in diameter. A double angle approach was used to reduce the effective diameter of the probe tip, see Fig. 4. The first angle was a little smaller than 10° and then the tip was finished with a 45° angle. The effective diameter of the tip, defined as the portion where the angle changes from 10° to 45°, was measured photographically using a microscope; it was a little less than 50 μm.

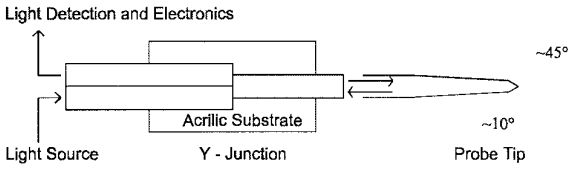

Fig. 4 - Outline of the local phase detection probe.

The setup of the probe was completed with a Y-junction made bonding the extremities of the fibers coming from the light source, the probe tip and the light detector, polished at 90 °, and then faced each other as shown in Fig. 4. To simplify the manufacture, a transparent acrylic substrate was used to house the fibers, which were then positioned using a microscope. Once positioned, the fibers were fixed in place with a drop of acrylic glue.

The light source was an He-Ne laser, 1 *mW* in power, focused on a polished tip of a fiber using a positioning mechanism. The light detection stage comprised a phototransistor, an amplifier and a comparator to generate both analog and digital outputs.

The probe tip was bare in its last 20 μm and then housed in a ceramic tube of 300 μm inner diameter, 500 μm outer diameter and 100 mm long. A positioning mechanism allowed the probe to be moved vertically in the two phase flow region.

EXPERIMENTAL RESULTS AND DISCUSSION

Heat Transfer and Critical Heat Flux

Linear power ramps (actually linear in I^2) were generated with a heat-up rate not higher than 0.3 $W/cm^2\ s$, well below the upper limit for negligible heat-up rate effects in the CHF on a wire [19], and also appropriate for the semi-cylindrical heater. This power ramps were used to simultaneously measure complete boiling curves up to the first boiling crisis and the CHF. From the boiling curves the heat transfer coefficient has been calculated.

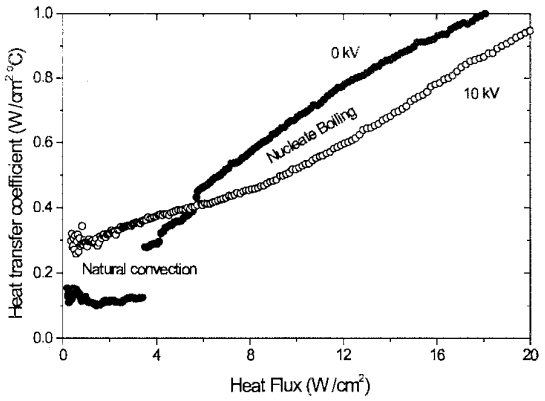

Fig. 5 - Effect of the heat transfer coefficient as a function of wall overheating for 0 kV and 10 kV of applied voltage (wire heater).

In Fig. 5 we show the heat transfer coefficient as a function of the wall overheating for the case of the wire heater, for 10 kV and without applied voltage. It can be clearly seen that there is an enhancement on the heat transfer in natural convection regime. The opposite trend, though to a less extent, can be seen in Fig. 6 for the case of adverse dielectrophoretic forces. These results confirm the findings of previous experimental works for favorable dielectrophoretic forces [5, 14] and is interesting to see that adverse electric fields cause a slight degradation of the heat transfer in natural convection. This kind of behavior was predicted by Maekawa et al. [20] who pointed out that for plane geometry, and under given conditions, it is possible to suppress natural convection. Notice also that, with an applied electric field and no matter the direction of the dielectrophoretic force, the onset of nucleate boiling is suppressed, resulting in a smooth transition from natural convection to bubble nucleation.

The effect of an imposed electric field on the nucleate boiling heat transfer is small, both in favorable and adverse electric fields. In favorable electric fields there is a slight enhancement of the heat transfer coefficient at low heat fluxes, but at high heat fluxes the heat transfer is degraded by the application of an electric field, as already pointed out in reference [14]. This behavior can be explained in terms of the very high increase of the heat transfer coefficient with the application of an electric field in the natural convection regime (the heat transfer coefficient increases threefold), which remains still important at low heat fluxes in nucleate boiling.

In the case of adverse electric fields there is no enhancement of the nucleate boiling heat transfer; the heat transfer coefficient with applied voltage remains smaller than without electric field for all the heat fluxes in nucleate boiling up to CHF. The reasons for this trend are unknown to us, but some conjectures can be made. The application of an adverse electric field pushes the bubbles toward the heater, thus allowing the bubbles to grow bigger. This has been verified visually. The consequences of this are probably the reduction of microconvection and of other heat transfer mechanisms in nucleate boiling such as evaporation-condensation at the bubble surface when attached to the heater [21].

CHF results for applied voltages from 0 to 10 kV and for favorable and adverse dielectrophoretic forces are shown in Fig. 7. The figure depicts data for saturated and subcooled CHF and are related to the CHF at zero imposed electric field. The data for favorable electric fields are taken from reference [7].

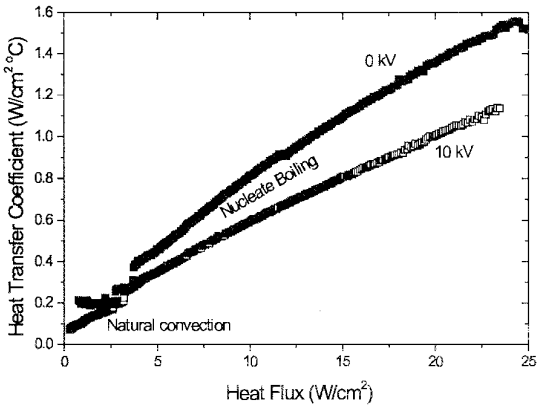

Fig. 6 - Effect of the heat transfer coefficient as a function of heat flux for 0 kV and 10 kV of applied voltage (semi-cylindrical heater).

The CHF greatly increases with the application of an electric field under favorable conditions, as already reported by other authors [5, 6, 14]. The effect of subcooling on the CHF is to reduce the effect of the presence of the electric field, as can be seen comparing the curves for saturation temperature to that with 26.7 °C of liquid subcooling. The experimental results from Di Marco and Grassi [22] indicate that the subcooling also reduces the effects of the electric field on the CHF, though to a smaller extent. In their paper they claim that the enhancing effect on CHF due to the effect of subcooling is independent on subcooling.

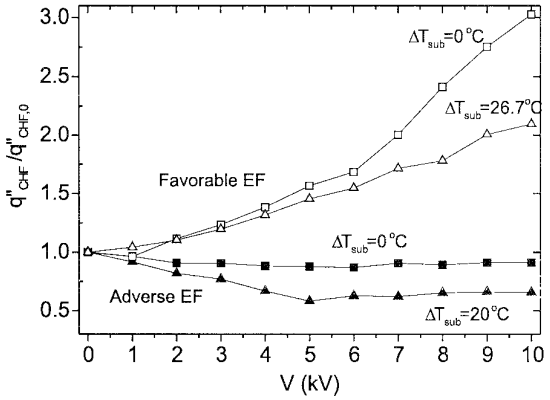

Fig 7 - Ratio between Critical Heat Flux with applied voltage to CHF with no voltage for favorable and adverse dielectrophoretic forces under saturated and subcooled conditions.

In opposition to the trend observed under favorable dielectrophoretic forces, an adverse dielectrophoretic force reduces the CHF considerably. To the knowledge of the authors, this degradation of the Critical Heat Flux under the effects of an externally imposed electric field has not been measured before. The generation of an adverse electric field gradient is by far more difficult than to create a favorable field gradient. This has been done in our case using a cylindrical geometry, though also a spherical geometry would be appropriate. However, the maximum realizable gradient of electric field is limited by the dielectric breakdown, so it was not possible to reach the field gradients that can be achieved with geometries

such as the wire heater. Reducing the heater radius the electric field over the surface of the cylinder increases, but the maximum attainable voltage before breakdown decreases. Under the experimental conditions of this work the semi-cylindrical heater was built as small as possible but trying to avoid bubble blockage by the electrode.

The effect of subcooling in the CHF under electric fields in the case of adverse dielectrophoretic forces is the opposite to that with favorable electric fields: the subcooling increases the effect of the presence of an electric field. In addition, there is a sort of saturation on the CHF for applied voltages beyond 5 kV, and even a slight increase in the case with a subcooling of 20 °C.

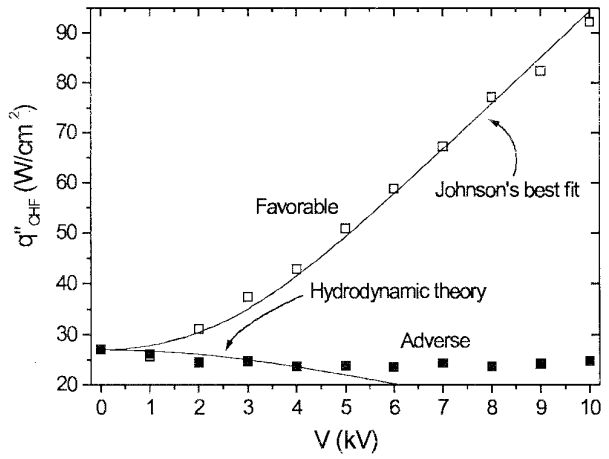

Fig. 8 - Critical Heat Flux versus applied voltage for favorable and adverse dielectrophoretic forces under saturated conditions.

Fig. 8 shows the effect of an applied electric field on the CHF for both favorable and adverse dielectrophoretic forces. The best fit of the CHF model of Johnson [3] is shown for the case of favorable electric field gradient. This model, based on the hydrodynamic instability theory, works well for the case of CHF on wires, as already pointed out in other works [6, 7, 14]. For the case of an adverse electric field gradients, the model of Berghmans [11], developed for cylindrical interfaces, was applied. Even though the model correctly predicts a reduction of the CHF with the applied voltage, it does not explain the presence of the saturation at certain electric field strength. Berghmans' model, also based on the hydrodynamic instability theory, may be subject to more refinements to predict the features found experimentally. Unfortunately no other models of CHF have been extended to the case with electric fields.

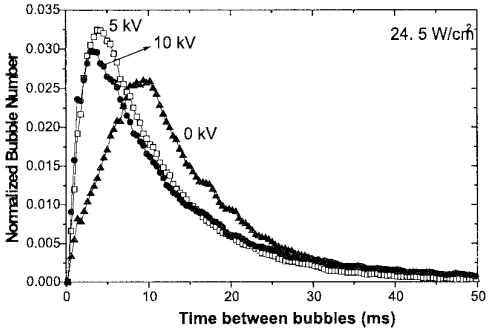

Fig 9 - Distribution of time between bubbles for nucleate boiling on a wire at different applied voltages.

Two-Phase Flow - Steady State Measurements

Local two-phase flow parameters have been measured over a heated using the phase-detection probe described in the previous section. From the digital signal of the single-tip probe the complete phase-indicator function was obtained as described in [16]. The phase-indicator function is defined as:

$$\chi(\vec{x},t)=\begin{cases}1 \text{ if vapor is present at the probe tip}\\ 0 \quad \text{otherwise}\end{cases} \tag{8}$$

and from it the vapor volume fraction at $\vec{x}$ can be calculated as

$$\alpha(\vec{x},t)=\frac{1}{\Delta t}\int_{t-\Delta t/2}^{t+\Delta t/2}\chi(\vec{x},\tau)d\tau \tag{9}$$

where is integration interval. The interfacial impact rate at the probe tip is

$$\dot{N}=\frac{N(\vec{x},t-\Delta t/2,t+\Delta t/2)}{\Delta t} \tag{10}$$

with $N(\vec{x}, t - \Delta t/2, t + \Delta t/2)$ the number of interfaces touching the probe tip between $t - \Delta t / 2$ and $t + \Delta t / 2$. In addition, important information can be extracted from the indicator function calculating the distributions of bubble chordal time and of time between bubbles [16]. The bubble chordal time gives an idea of the ration between bubble size and bubble velocity, and the time between bubbles of the detachment frequency.

Fig. 9 shows the distribution of time between bubbles in nucleate boiling on a wire with 0, 5 and 10 *kV* of applied voltage. The heat flux for all three cases was 24.5 *W/cm*^{2}. Each curve was measured in steady-state conditions at 2.5 *mm* from the heater surface and the indicator function was composed by some 50,000 bubbles. From the figure it is evident that an increase on the electric field strength results in a shorter time between bubbles, and therefore in a higher bubble detachment frequency. This increase coexists with a reduction on the bubble detachment size, as visually and photographically observed in this and other works [6, 14].

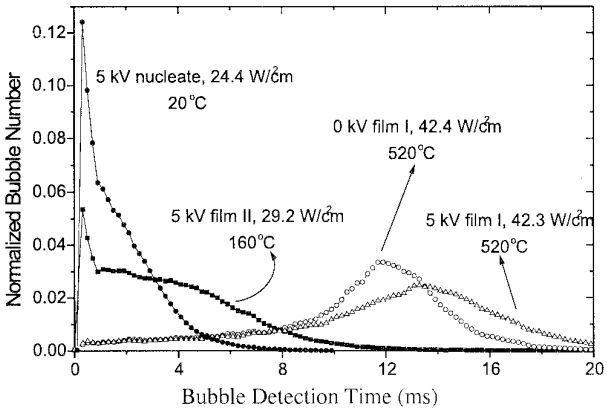

Fig. 10 - Distribution of bubble detection time (or bubble chordal time) for nucleate and the two regimes of film boiling on a wire.

The bubble chordal time distributions for nucleate boiling and the two regimes of film boiling at 5 *kV* of applied voltage are shown in Fig. 10. The case of film boiling at 0 *kV* is also shown. The curves for film I show clearly that the effect of an applied voltage on the distribution is small, the curve moves somewhat toward larger times, indicating either larger or slower bubbles. The wire temperature is not modified by the application of an electric field in this regime.

The visual observation of the film II regime resembles the nucleate boiling regime. The big difference is the heater temperature, that in the case shown in the figure rises from 20 °*C* to 160 °*C*. We can see in Fig. 10 that the bubble time distribution for film II is considerably wider than that for nucleate boiling, and that we have much more large bubbles and less small bubbles. However, the film II regime is much closer to nucleate boiling than to film I.

Two-Phase Flow – Transient Measurements

Experiments with linear power cycles of 20 *s* period were performed. The maximum heat flux on each cycle was about 35 W/cm^2 for 0 kV of applied voltage and 50 W/cm^2 for 5 kV. This heat flux was just high enough to guarantee all the boiling regimes to be present on the cycle. To avoid extreme excursions of power on the transitions, a constant voltage power control was adopted [14]. Two sets of measurements were performed to asses repeatability, each with 50 cycles. These were then averaged and processed to obtain instantaneous ensemble averaged values of impact rate and void fraction as described in [23].

Fig. 11 shows the evolution of an ensemble average on the impact rate-void fraction plane for a set of power cycles at no external electric field. As the power increases, the cycle follows the arrow in a clockwise fashion. We can see that the void fraction and impact rate increase in nucleate boiling up to a point in which the interfacial impact rate decreases strongly and the void fraction has a slight reduction. This can be due to the bubble size increase that occurs just before CHF. After a short period in transition boiling the film boiling I regime takes place. In this regime the impact rate shows almost no variation with the heat flux, indicating that the detachment frequency remains rather constant and only the bubble size changes, resulting in important changes on the void fraction. Once the point of Leidenfrost is reached, the system returns to nucleate boiling.

The behavior is somewhat different when an electric field is applied. In the nucleate boiling region the qualitative shape is the same, but the impact rate is considerably higher when an electric field is applied, in this case rises from a maximum of about 140 *Hz* without electric field to 245 *Hz* with 5 *kV* of applied voltage. Once the transition to film boiling occurs, the system tends to set to film II regime, but due to the transient increasing power film I establishes. The system remains a while in film boiling I regime, characterized by high void fraction and low impact rate, and then the transition to film boiling II occurs.

The film boiling II regime has an impact rate higher and a void fraction smaller than film I. Even though the differences between the film I and film II regimes can be clearly noticed, the setting of the regimes on the wire is rather diffuse due to the appearance of two-mode, and even three mode boiling caused by the voltage control instead of current control [14]. This can be avoided using current control, but in that case the 0.2 *mm* wire cannot resist a sufficient number of cycles to perform reasonable averages. In any case, Figs. 11 and 12 show the qualitative behavior of the two-phase flow parameters.

Two-Phase Flow - Spatial Measurements

Spatial measurements of interfacial impact rate and void fraction were made moving the probe tip vertically from 0.5 to 5 *mm* from the heater, keeping a vertical line centered respect to the heater.

Figs. 13 and 14 show the variation of the void fraction on nucleate boiling for heat fluxes of 15 and 23 *W/cm*^{2} and for applied voltages of 0 and 5 *kV* as a function of the distance to the heater. The number of interfaces measured was about 100,000 (50,000 bubbles).

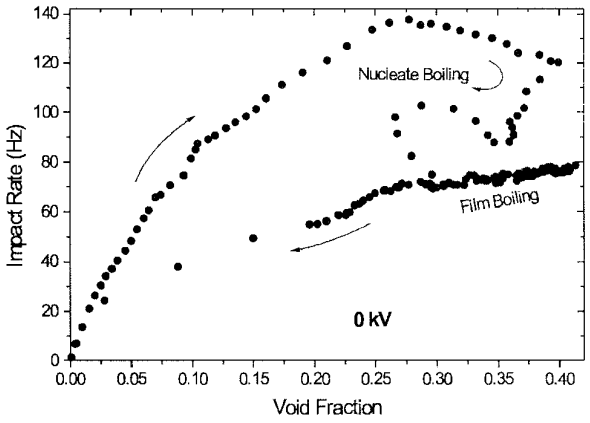

Fig. 11 - Evolution of an ensemble average on the impact rate-void fraction plane for a set of power cycles at no external electric field.

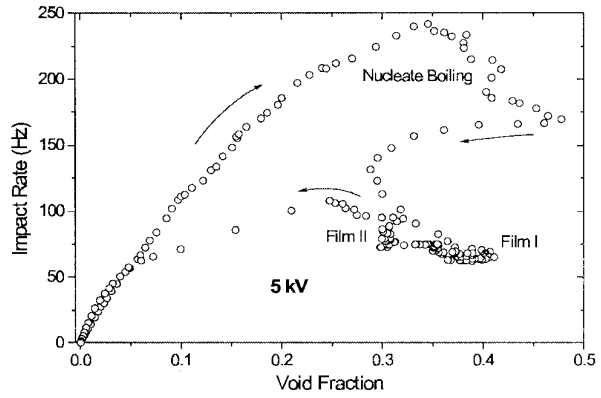

F. 12 - Evolution of an ensemble average on the impact rate-void fraction plane for a set of power cycles at 5 *kV* applied voltage.

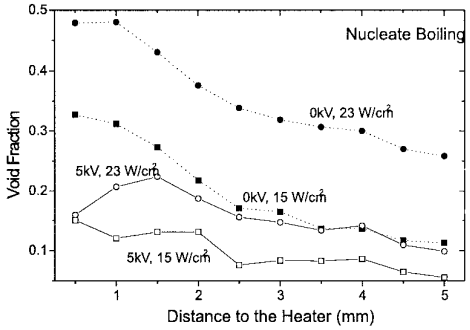

Fig. 13 - Void fraction on nucleate boiling for different heat fluxes and applied voltages as a function of the distance to the heater.

For both heat fluxes, the void fraction is higher when no electric field is applied. Conversely, the interfacial impact rate is higher near the heater with electric field but decays faster as we move away from the heated surface. This effect is probably due to the radial nature of the dielectrophoretic force that helps the dispersion of the plume, thus reducing the number of bubbles impacting the probe tip as we move away from the heater. Large coalescence rates could also be responsible for this trend.

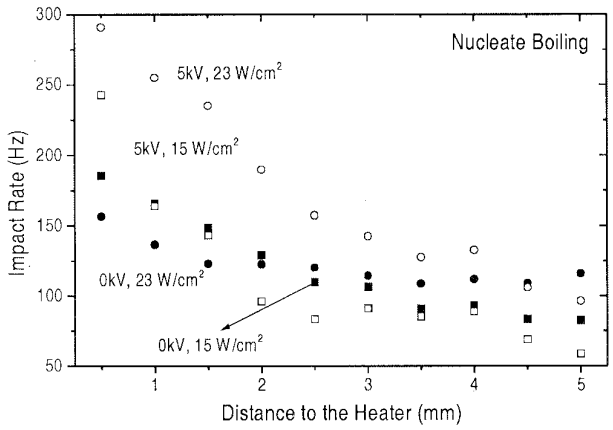

Fig. 14 - Impact rate on nucleate boiling for different heat fluxes and applied voltages as a function of the distance to the heater.

The peak on the void fraction that tends to develop near the wall is suggesting and was already observed for pool boiling over an horizontal heater without electric fields [23]. Interestingly, the peak is more noticeable when an electric field is applied. No satisfactory explanation to this phenomenon has been found even for the case without electric fields.

Measurements were also made in film boiling under diverse conditions. The minimum distance to the heated wall was in this case 1 *mm* for film boiling II and 1.5 *mm* for film boiling I. This distance was the minimum that resulted in no damage to the plastic probe tip by the high temperatures present in film boiling. The number of interfaces measured was about 50,000 for each experimental point, 50 % less than in the case of nucleate boiling because the impact rate is considerably smaller and then the acquisition time becomes too long.

Fig. 15 shows the void fraction as a function of the distance to the heater for the different film boiling regimes, at two heat fluxes and, for the case of film boiling I, for 0 and 5 *kV* of applied voltage. Three different sets of measurements were taken to assess repeatability and then the three curves were averaged. The same procedure was followed for Fig. 16, that shows the interfacial impact rate.

In all cases the void fraction decreases with the distance to the heater, with a faster decay on film I. As expected, the void fraction increases with the heat flux, both with and without applied electric field. The application of an electric field slightly reduces the void fraction, and much smaller values of void fraction occur in film II as compared to film I, though in the figure the heat fluxes are not the same (28.1 *W/cm²* for film II, 36.3 *W/cm²* for film I). The interfacial impact rate has exactly the opposite trend: it is higher in film II than in film I, as can be seen in Fig. 16. In addition, the interfacial impact rate in film I slightly increases with the distance to the heater, possibly due to bubble breakup.

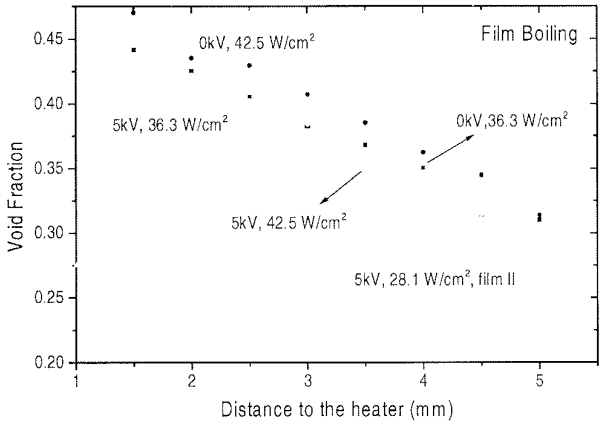

Fig. 15 - Void fraction on film boiling for different heat fluxes and applied voltages as a function of the distance to the heater.

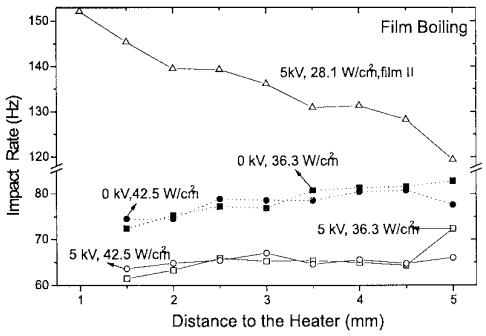

Fig.16 - Impact rate on film boiling for different heat fluxes and applied voltages as a function of the distance to the heater.

CONCLUSIONS

An experimental study of boiling heat transfer and critical heat flux enhancement and degradation has been presented. The study includes measurements of two-phase flow parameters (void fraction and interfacial impact rate) during each of the boiling regimes and during the regime transitions.

The main conclusions of this work can be summarized as follows:

- *Critical heat flux*: There is a strong increase on the CHF under electric field gradient that cause favorable dielectrophoretic forces. This is the case when the heater is a wire with a cylindrical outer electrode. On the other hand, the CHF decreases when we apply an electric field gradient that causes adverse dielectrophoretic forces. Reduction of about 40 % were measured for applied voltages of 5 *kV* and 20 *°C* of subcooling.

- *Nucleate boiling heat transfer*: there is a small degradation of the heat transfer at high heat fluxes both with favorable and adverse dielectrophoretic forces, as compared to the case without electric fields. At low heat fluxes there is an (also small) increase of the heat transfer coefficient.

- *Natural convection*: a strong enhancement of the heat transfer in natural convection is observed when a favorable electric field is applied. When the electric field is adverse the effect of an applied voltage is a small degradation of the heat transfer or negligible.

• *Two-phase flow*: the two-phase flow study shows that the second film boiling regime has a two-phase structure more similar to that of nucleate boiling than to film boiling. The interfacial impact rate in film boiling II is much higher than in film boiling I, similar to the results for nucleate boiling.

ACKNOWLEDGEMENTS

The help provided by Mr. Daniel Mateos Bickel for the setup of the experiments is deeply acknowledged.

REFERENCES

[1] M. Markels and R. L. Durfee, "The Effect of Applied Voltage on Boiling Heat Transfer", *AIChE J.* **10**, 106-110 (1964)

[2] M. Markels and R. L. Durfee, "Studies of Boiling Heat Transfer with Electrical Fields", *AIChE J.* **11**, 716-723 (1965)

[3] R. L. Johnson, "Effect of an Electric Field on Boiling Heat Transfer", *AIAA J.* **6**, 1456-1460 (1968)

[4] A. G. Zhorzholiani and I. G. Shekriladze, "Study of the Effect of an Electrostatic Field on Heat Transfer with Boiling Dielectric Fluids", *Heat Transfer-Soviet Res.* **4**, 81-98 (1972)

[5] T. B. Jones, "Electrohydrodynamically Enhanced Heat Transfer in Liquids-a Review", *Advances in Heat Transfer* **14**, 107-148 (1978)

[6] P. Di Marco and W. Grassi, "Saturated Pool Boiling Enhancement by Means of an Electric Field", *Enhanced Heat Transfer* **1**, 99-114 (1993)

[7] V. Masson and P. M. Carrica, "Effects of an Externally Imposed Electric Field on Subcooled Boiling Critical Heat Flux", *Int. Comm. Heat Mass Transfer* 22, 483-492 (1995)

[8] N. F. Baboi, M. K. Bologa and A. A. Klyukanov, "Some Features of Ebullition in an Electric Field, *Appl. Elec. Phenomena (USSR)* 20, 57-70 (1968)

[9] P. M. Carrica, P. Di Marco and W. Grassi, "Electric Field Effects on Film Boiling on a Wire", *Exp. Heat Transfer* 9, 11-27 (1996)

[10] N. Zuber, "Hydrodynamic Aspects of Boiling Heat Transfer", *Atomic Energy Comission Report AECU-4439* (1959)

[11] J. Berghmans, "Electrostatic Fields and the Maximum Heat Flux", *Int. J. Heat Mass Transfer* 19, 791-797 (1976)

[12] P. M. Carrica, P. Di Marco and W. Grassi, "Nucleate Pool Boiling in the Presence of an Electric Field: Effect of Subcooling and Heat-up Rate", *Exp. Thermal Fluid Sci.* 15, 213-220 (1997)

[13] P. Di Marco and W. Grassi, "EHD Effects on Pool Boiling in Reduced Gravity", to be presented at the *5th ASME-JSME Thermal Engineering Joint Conference*, San Diego, USA (1999)

[14] P. M. Carrica, P. Di Marco and W. Grassi, "Effect of an Electric Field on Nucleate Pool Boiling and Critical Heat Flux: Overview of the Results of an Experimental Study", *Proc. IV ASME/JSME Thermal Engineering Joint Conf.*, Maui, HI, USA (1995)

[15] M. Uemura, S. Nishio and I. Tanasawa, "Enhancement of Pool Boiling Heat Transfer by Static Electric Field", *9th Int. Heat Transfer Conf.*, Jerusalem, 4, 75-80 (1990)

[16] P. M. Carrica, V. Masson and P. Di Marco, "Application of a Low Cost True-Monofiber Local Phase Detection Probe to Void Fraction Measurements in Pool Boiling", *4th World Conf. on Exp. Heat Transfer, Fluid Mech. and Thermodynamics*, Brussels, Belgium (1997)

[17] UNI (Italian Standard Agency) Platinum Wire Thermometers, Standard Table nº 7397 (in Italian) (1979)

[18] V. Masson, "Estudio de Algunos Efectos del Campo Eléctrico en la Ebullición de Líquidos Dieléctricos", Degree Thesis in Physics, Universidad Nacional de Mar del Plata, Argentina (In Spanish) (1995)

[19] P. M. Carrica, P. Di Marco & W. Grassi, "Nucleate Pool Boiling in the Presence of an Electric Field: Effects of subcooling and heat-up rate", *Experimental Thermal and Fluid Science* 15, 213-219 (1997)

[20] T. Mackawa, K. Abe and I. Tanasawa, "Onset of Natural Convection under an Electric Field", *Int. J. Heat Mass Transfer* 35, 613-621 (1992)

[21] S. Van Stralen and R. Cole, *Boiling Phenomena*, Hemisphere Pub. Co., NY (1979)

[22] P. Di Marco and W. Grassi, "Combined Effect of Electric Field, Subcooling and Microgravity on Critical Heat Flux on a Wire in Pool Boiling", *Int. Eng. Foundation Conf. on Convective Flow and Pool Boiling*, Kloster Irsee, Germany, May 18-23 (1997)

[23] P. M. Carrica, S. Leonardi and A. Clausse, "Experimental Study of the Two-Phase Flow Dynamics in Nucleate and Film Boiling", *Int. J. Multiphase Flow* 21, 405-418 (1995)